

# Superconductivity in tantalum self-intercalated $4Ha$ - $Ta_{1.03}Se_2$

Hua Bai<sup>1</sup>, Mengmeng Wang<sup>1</sup>, Xiaohui Yang<sup>1</sup>, Yupeng Li<sup>1</sup>,  
Jiang Ma<sup>1</sup>, Xikang Sun<sup>1</sup>, Qian Tao<sup>1</sup>, Linjun Li<sup>2</sup>, Zhu-An  
Xu<sup>1,3,4,5</sup>§

<sup>1</sup>Department of Physics, Zhejiang University, Hangzhou 310027, P. R. China

<sup>2</sup>State Key Laboratory of Modern Optical Instrumentation, College of Optical Science and Engineering, Zhejiang University, Hangzhou 310027, China

<sup>3</sup>State Key Lab of Silicon Materials, Zhejiang University, Hangzhou 310027, P. R. China

<sup>4</sup>Zhejiang California International NanoSystems Institute, Zhejiang University, Hangzhou 310058, P. R. China

<sup>5</sup>Collaborative Innovation Centre of Advanced Microstructures, Nanjing 210093, P. R. China

E-mail: zhuan@zju.edu.cn

**Abstract.**  $TaSe_2$  has several different polytypes and abundant physical properties such as superconductivity and charge density waves (CDW), which had been investigated in the past few decades. However, there is no report on the physical properties of  $4Ha$  polytype up to now. Here we report the crystal growth and discovery of superconductivity in the tantalum self-intercalated  $4Ha$ - $Ta_{1.03}Se_2$  single crystal with a superconducting transition onset temperature  $T_c \approx 2.7$  K, which is the first observation of superconductivity in  $4Ha$  polytype of  $TaSe_2$ . A slightly suppressed CDW transition is found around 106 K. A large  $\mu_0 H_{c2}/T_c$  value of about 4.48 is found when magnetic field is applied in the  $ab$  plane, which probably results from the enhanced spin-orbit coupling (SOC). Special stacking faults are observed, which further enhance the anisotropy. Although the density of states at the Fermi level is lower than that of other polytypes,  $T_c$  remains the same, indicating the stack mode of  $4Ha$  polytype may be beneficial to superconductivity in  $TaSe_2$ .

§ Corresponding author. Tel: (86)571-87953255 E-mail address: zhuan@zju.edu.cn (Z.A.Xu)

## 1. Introduction

Transition metal dichalcogenides (TMDCs) are the  $TX_2$ -type compounds ( $T$  = transition metal,  $X$  = S, Se, Te), which exhibit many fascinating properties, such as superconductivity [1], CDW [2], large magnetoresistance [3], and topological semimetals [4], etc. TMDCs have a layered structure, in which each layer consists of a  $X - T - X$  sandwich. The sandwich have two different types: octahedral and trigonal. The layers are coupled by van der Waals forces. Due to different sandwich types and different stack modes, TMDCs often have many polytypes [5], such as  $1T$ ,  $2Ha$ ,  $2Hb$ ,  $3R$ , etc. The number dictates the layers number in one unit cell, and the capital letter represents crystal system, i.e.,  $T$  is tetragonal,  $H$  is hexagonal, and  $R$  is rhombohedral. Hexagonal TMDCs also have different types, therefore use the lowercase letter to distinguish them. In TMDCs, the modulation of CDW state always lead to interesting phenomenon. For instance, with Cu intercalation or electric-field gating effect, the CDW transition of  $1T-TiSe_2$  can be suppressed and superconductivity appears [6, 7]. By gate-controlled Li ion intercalation,  $1T-TaS_2$  thin flakes undergo multiple phase transitions including the transition from the Mott insulator to superconductor [8]. In  $2Ha-TaS_2$ , pressure suppresses CDW transition and superconducting  $T_c$  is significantly enhanced [9].

$1T-TaSe_2$  undergoes an incommensurate-charge-density waves (ICCDW) phase transition at  $T_{ICDW} \approx 473$  K, and no superconducting transition is observed [10]. With S or Te doping, superconductivity appears [11–13].  $2Ha-TaSe_2$  also undergoes an ICCDW phase transition at  $T_{ICDW} \approx 122$  K, then locks-in to a commensurate-charge-density waves (CCDW) state at  $T_{CCDW} \approx 90$  K [14, 15], and finally to a superconducting state at  $T_c \approx 0.14$  K [16, 17].  $T_c$  will increase with S or Te doping [18, 19], or Ni or Pd intercalations [20, 21], or under pressure [9].  $3R-TaSe_2$  is not stable [22], but with Te, Mo or W doping, it becomes stable and superconducting at  $T_c$  of about 2 K [23].  $4Hb-TaSe_2$  also has two different CDW phase transitions at 410 K and 75 K respectively [24], and  $6R-TaSe_2$  has the similar behavior [25]. In  $4Hb-TaS_{2-x}Se_x$  ( $0 \leq x \leq 1.5$ ) and  $6R-TaS_{2-x}Se_x$  ( $0 \leq x \leq 1.6$ ), superconductivity and CDW coexist in whole composition range [26, 27]. Nevertheless for  $4Ha-TaSe_2$ , there is few reports on its physical properties up to now, most likely because this polytype is difficult

to synthesis.

Here we report the successful crystal growth and superconductivity in Ta self-intercalated  $4Ha-Ta_{1.03}Se_2$  single crystal.  $T_c$  of  $4Ha-Ta_{1.03}Se_2$  is about 2.7 K, which is approximately 20 times higher than that of  $2H-TaSe_2$ , close to the  $T_c$  value reported for other doped or intercalated polytypes. We also found a phase transition around 106 K, which is analogous to a slightly suppressed CDW transition. A large  $\mu_0 H_{c2}/T_c$  value of about 4.48 is found when magnetic field is applied in the  $ab$  plane which may be related to the enhanced spin-orbit coupling (SOC).

## 2. Experiment Details

Single crystals of  $4Ha-Ta_{1.03}Se_2$  were made via vapor transport technique using iodine as the transport agent. First, Ta(99.99%) and Se(99.999%) powder were mixed with the ratio of 1.06:2 and ground adequately, sealed into an evacuated quartz ampoule, heated to 800 °C and kept for 3 days. Subsequently, the mixture was reground and added with iodine in a concentration of 8.6 mg/cm<sup>3</sup>, sealed into an evacuated quartz ampoule with a length of 16 cm. The ampoule was heated for 7 days in a two-zone furnace, where the temperature of source zone and growth zone were fixed at 850 °C and 800 °C respectively. Finally, the silver, mirror-like plates single crystals with typical size of about  $4 \times 4 \times 0.05$  mm<sup>3</sup> were obtained. We also tried to fabricate the stoichiometric  $4Ha-TaSe_2$  with the same method but failed. We guess that the redundant Ta atoms conduce to the formation of  $4Ha$  polytype.

The single crystal X-ray diffraction (XRD) data were collected by a PANalytical X-ray diffractometer (Empyrean) with a Cu  $K_\alpha$  radiation and a graphite monochromator at room temperature. The chemical compositions were determined by energy-dispersive X-ray spectroscopy (EDX) with a GENESIS4000 EDAX spectrometer. High-resolution transmission electron microscope (HRTEM) images were taken at room temperature with an aberration corrected FEI-Titan G2 80-200 ChemiSTEM. DC magnetization was measured on a magnetic property measurement system (MPMS-XL5, Quantum Design), and the “Ultra Low Field” option was used. The specific-heat capacity was measured on a physical properties measurement system (PPMS-9, Quantum Design), using a relaxation technique. The electrical properties were measured

on an Oxford Instruments-15T cryostat with a He-3 probe.

### 3. Result and Discussion

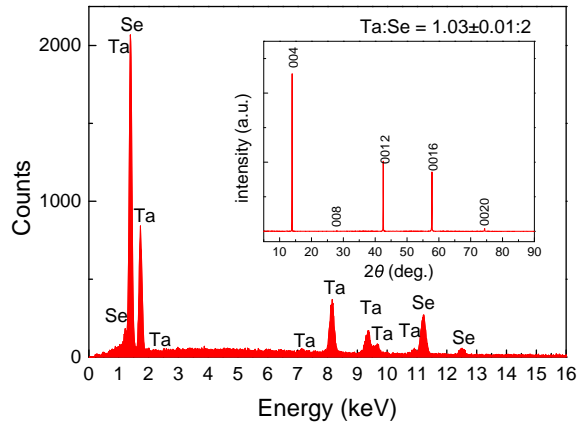


**Figure 1.** EDX pattern of  $4Ha-Ta_{1.03}Se_2$ . Inset: XRD pattern of a  $4Ha-Ta_{1.03}Se_2$  single crystal.

Figure 1 shows the EDX pattern of the single crystal. The ratio of Ta to Se is determined to be 1.03(1):2, which is an average result for multiple areas in the same single crystal. Although the starting ratio is 1.06:2, the redundant amount of Ta atom are not all intercalated into the sample. We get similar results for several batches under the same condition. The room temperature XRD pattern of a  $4Ha-Ta_{1.03}Se_2$  single crystal is shown in the inset of Figure 1, where all the reflections are  $(00l)$  peaks. The lattice constant along the  $c$ -axis is calculated to be 25.436 Å. Comparing with 25.180 Å of  $4Ha-TaSe_2$  from the literature [28], the  $c$ -axis is a little expanded. This should result from the Ta self-intercalation, similar to the Ni or Pd intercalated  $2H-TaSe_2$  [20, 21].

The structure model is displayed in Figure 2(a), and Figure 2(b) and (c) shows the HRTEM images of a single crystal from zone axes  $[100]$ . The HRTEM images clearly reveal the atoms arrangement mode and thus provide a direct evidence for the  $4Ha$  polytype. Every 4 layers constitute one unit cell. The layer stacking type can be described by using the method from the literature [5], where A(a), B(b), C(c) represent three positions of atoms in the  $ab$ -plane. The capital letters correspond to the Se atoms and the lower case letters designate the Ta atoms. The same letters, no matter capital or lower case, represent the same positions in the  $ab$ -plane for all layers. Every three letters describe one sandwich layer. Along the  $c$ -axis, the stacking sequence of  $4Ha$  polytype is AbACbCBaBCbC, just as illustrated in the left structure in Figure 2(a). The HRTEM images

also reveal special stacking faults in our samples as displayed in Figure 2(a). Both A block and B block consist of 4 layers of the  $4Ha-TaSe_2$  structure, but from different sections and directions as shown in Figure 2(a). Our sample is randomly stacked by the A and B blocks. These stacking faults could enhance the anisotropy due to the 2-dimensional characteristic of fragments. Moreover, the intercalated Ta atoms between two layers can be clearly observed in the locally enlarged HRTEM image as shown in Figure 2(c). It can be found that the Ta intercalation is microscopically not homogeneous.

Figure 3(a) displays the temperature dependence of in-plane electrical resistivity for  $4Ha-Ta_{1.03}Se_2$  single crystals. The sample was cut to a size of about  $4 \times 1 \times 0.05 \text{ mm}^3$  for the resistivity measurement. Similar to other polytypes,  $4Ha-Ta_{1.03}Se_2$  are metallic in normal state. Around 106 K, a slope change appears. This change can be better observed in the derivative of resistivity curve as shown in the inset. Below 106 K, there is a suddenly increase in the derivative of resistivity curve. This slope change is analogous to the case in other TMDCs and usually it is attributed to the CDW transitions [21]. The onset superconducting transition temperature  $T_c$  is about 2.7 K, with a narrow transition width of about 0.2 K. For other polytypes, when doping or intercalating,  $T_c$  is always in the range of 2 - 4 K. Although  $4Ha$  polytype has a disparate stacking pattern, the superconducting transition temperature remains similar to the others. Figure 3(b) shows the results of magnetic measurements. The inset is the field dependence of initial part of magnetization curve at 2 K with magnetic field applied parallel to the long direction in the  $ab$ -plane. The lower critical field ( $H_{c1}$ ) is estimated to be about 3 Oe. Thus we measured the temperature dependence of dc magnetic susceptibility under magnetic field of 1 Oe applied in the  $ab$ -plane. It was measured for both zero-field cooling (ZFC) and field cooling (FC). The  $T_c$  determined from magnetic susceptibility is 2.7 K, close to the onset temperature derived from the resistivity transition. The estimated superconducting shielding volume fraction is about 42.2% at 2 K. As mentioned above, the Ta intercalation is microscopically not homogeneous, therefore we conjecture that intercalation concentration is important for the occurrence of superconductivity, i.e., only the area with enough intercalated Ta atoms will show superconductivity.

Figure 4(a) and (b) display the temperature dependence of in-plane electrical resistivity under different magnetic fields of  $4Ha-Ta_{1.03}Se_2$  with field applied parallel to the  $c$ -axis and in the  $ab$ -plane respectively. For both field directions, the resistivity curves shift parallel down towards the low temperature with the increasing fields. This behavior is different

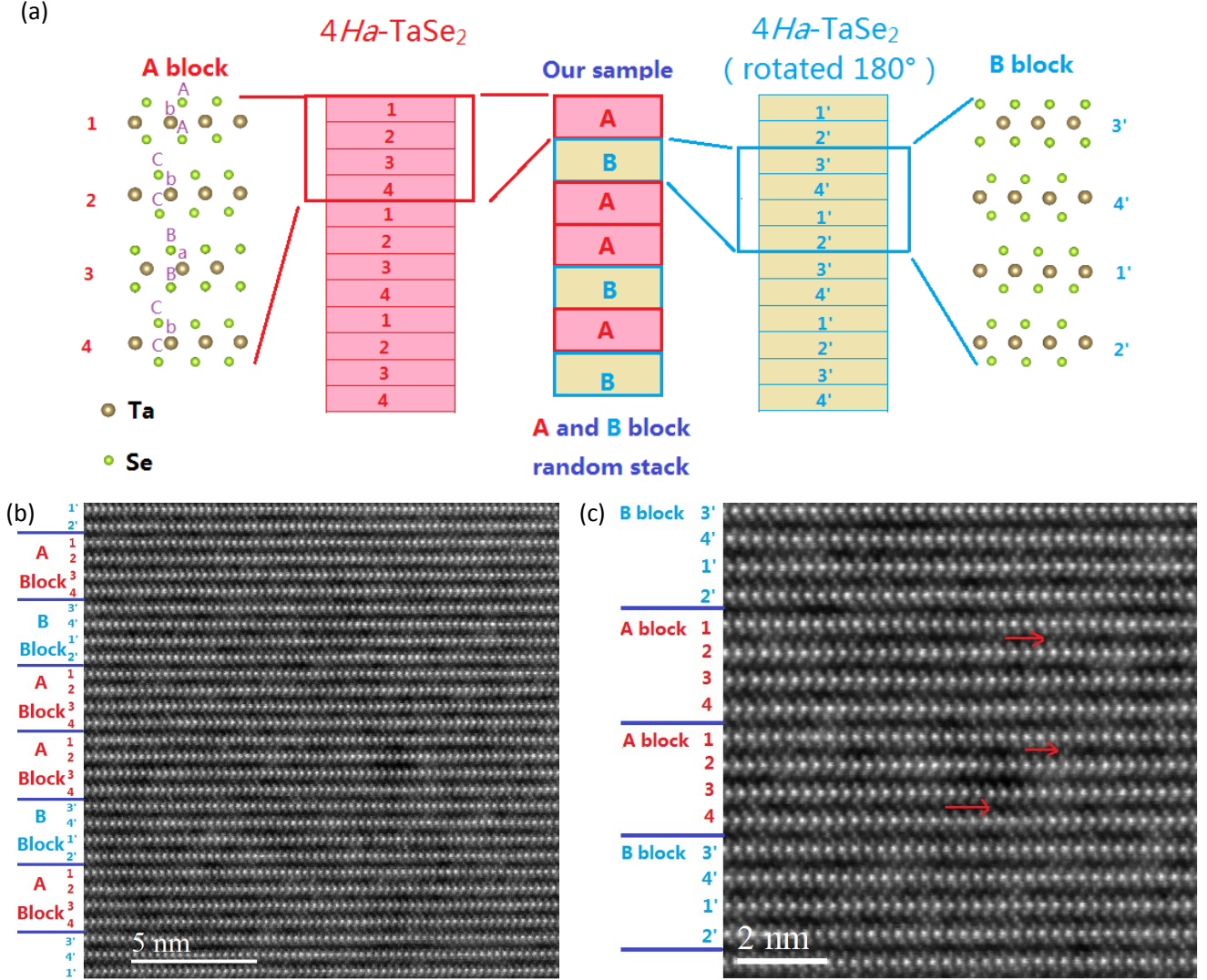


**Figure 2.** (a) The structure of  $4Ha$  polytype and the illustration for the special stacking faults in our samples. The purple letters in the left structure illustrate the stacking sequence of  $4Ha$  polytype. The right structure of  $4Ha-TaSe_2$  is rotated  $180^\circ$  along the  $c$ -axis. (b) HRTEM image of a  $4Ha-Ta_{1.03}Se_2$  single crystal from zone axes  $[100]$ . (c) Locally enlarged HRTEM image. The red arrows point out some of the intercalated Ta atoms.

from intercalated  $2H-TaSe_2$  whose resistive transition broadens when magnetic field is applied out of the  $ab$ -plane [21]. We summarize the temperature dependent upper critical field ( $H_{c2}$ ) determined by  $T_c^{\text{onset}}$  (90% of normal state resistivity) in Figure 4(c). In both directions, the  $H_{c2}$  data can be well fit by the Ginzberg-Landau (GL) equation [29]:

$$H_{c2}(T) = H_{c2}(0) \left( \frac{1-t^2}{1+t^2} \right) \quad (1)$$

where  $t = T/T_c$  is the reduced temperature. From this fit we can deduce  $\mu_0 H_{c2}(0) = 1.51$  T and  $\mu_0 H_{c2}^{ab}(0) =$

12.09 T. The Pauli paramagnetic limit for the upper critical field is  $\mu_0 H_P = 1.84 T_c = 4.96$  T.  $H_{c2}^{ab}(0)$  is about  $2.44 H_P$ , where  $\mu_0 H_{c2}^{ab}(0)/T_c = 4.48$ . For  $2H-TaSe_2$ ,  $H_{c2}$  is much smaller than Pauli paramagnetic limit for both directions, and  $\mu_0 H_{c2}^{ab}(0)/T_c = 0.03$  only [17]. However, for the Pd intercalated  $2H-Pd_{0.09}TaSe_2$ ,  $\mu_0 H_{c2}^{ab}(0)/T_c = 3.75$  [21], just slightly lower than the value in this work. Such a large value of  $\mu_0 H_{c2}(0)/T_c$  was also found in quasi-one-dimensional  $Nb_2PdS_5$  where the value is 3 [30], and in Pt, Ir or Ru doped  $Nb_2PdS_5$  where  $\mu_0 H_{c2}(0)/T_c$  increases due to additional SOC effect [31, 32]. We speculate that

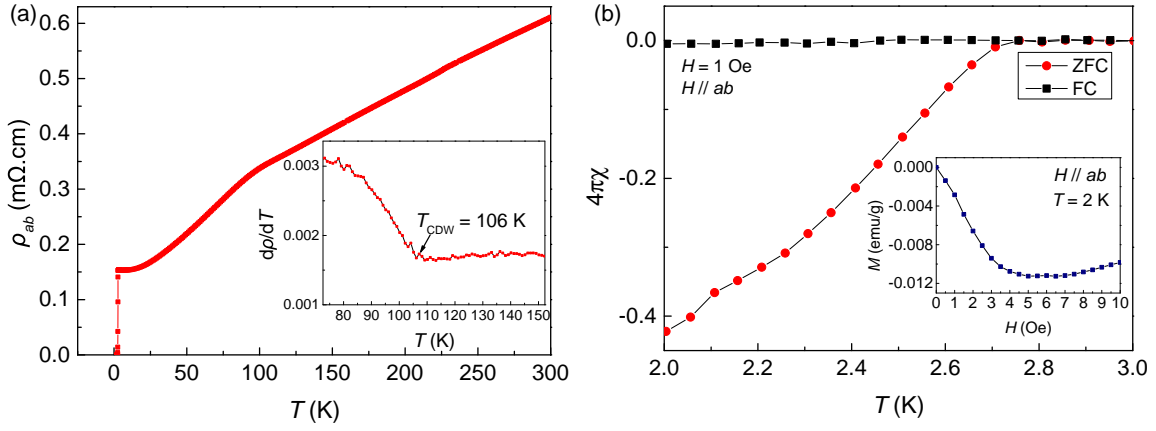


**Figure 3.** (a) Temperature dependent in-plane resistivity of  $4H\text{-Ta}_{1.03}\text{Se}_2$  for 1.5 - 300 K. Inset: Derivative of resistivity of  $4H\text{-Ta}_{1.03}\text{Se}_2$ . (b) Temperature dependence of dc magnetic susceptibility for  $4H\text{-Ta}_{1.03}\text{Se}_2$  ( $H//ab$ ,  $H = 1$  Oe). ZFC and FC denote zero-field cooling and field cooling. Inset: The field dependence of initial part of magnetization curve ( $H//ab$ ,  $T = 2$  K).

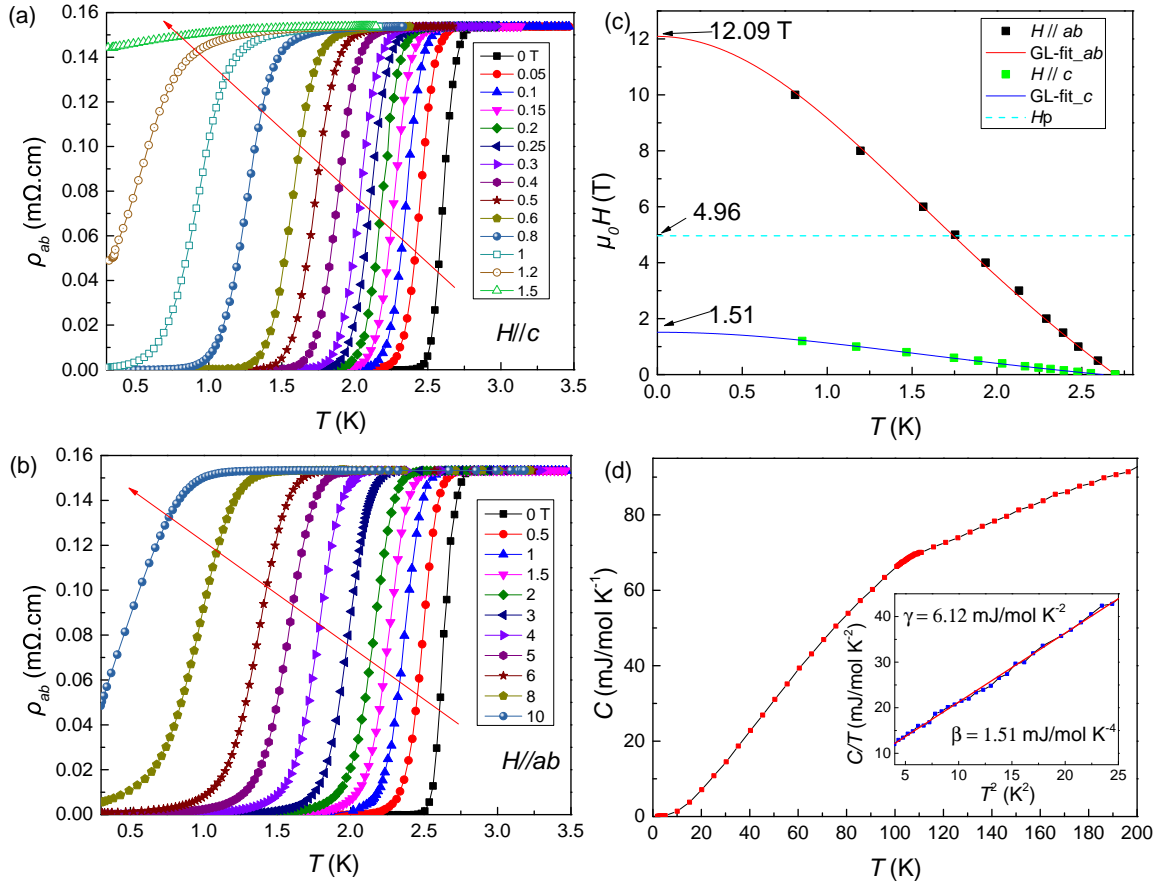


**Figure 4.** (a) (b) The resistivity under different magnetic fields from 0.3 - 3.5 K for  $4H\text{-Ta}_{1.03}\text{Se}_2$ . (a)  $H//c$ , up to 1.5 T. (b)  $H//ab$ , up to 10 T. (c) The upper critical field and the G-L fits for both field directions. The dash cyan line dictates the Pauli paramagnetic limit. (d) Temperature dependence of specific heat from 1.8 K - 200 K for  $4H\text{-Ta}_{1.03}\text{Se}_2$ . Inset: Low temperature part of specific heat divided by temperature, ( $C/T$ ), as a function of  $T^2$ , and the red line is a linear fit.

in  $\text{TaSe}_2$ , extra Ta atoms may resemble the effect to increase SOC, hence lead to the large upper critical fields. The anisotropy factor  $\gamma = H_{c2}^{ab}(0)/H_{c2}^c(0) \approx$

8, which is larger than the value of about 3 - 4 for  $2H$  polytypes [17, 21]. As mentioned above, the special stacking faults may also contribute to such large

anisotropy.

Figure 4(d) shows the temperature dependence of specific-heat  $C(T)$  for  $4Ha-Ta_{1.03}Se_2$  from 1.8 K to 200 K. No distinct specific-heat jump is observed for the CDW transition around 106 K. Combining with the minimum in derivative curvature of resistivity, we can conclude that the CDW transition has been severely suppressed by Ta-self intercalation in  $4Ha-Ta_{1.03}Se_2$ . This phenomenon is similar to  $2H-Ni_{0.02}TaSe_2$  [20] where there is an anomaly in temperature dependent resistivity but not in the specific-heat. Moreover, similar to  $2H-Ni_{0.02}TaSe_2$ , there is no obvious specific-heat jump around  $T_c$ , which may be due to the low volume fractions of magnetic shielding. The  $C/T$  versus  $T^2$  curve is displayed in the insert of Figure 4(d). The data can be well fit by the equation  $C/T = \gamma + \beta T^2$ , where  $\gamma$  is Sommerfeld coefficient for electronic specific-heat and  $\beta$  is lattice specific-heat coefficient. From the fit results we can obtain  $\gamma = 6.12$  mJ/mol  $K^{-2}$  and  $\beta = 1.51$  mJ/mol  $K^{-4}$ . Furthermore, we can estimate the Debye temperature  $\Theta_D$  by the formula  $\Theta_D = (12\pi^4 n R / 5\beta)^{1/3} = 157.42$  K, where  $n$  is the number of atoms per formula unit ( $n = 3.03$ ), and  $R$  is the gas constant. The electron-phonon coupling constant  $\lambda_{e-ph}$  can be estimated by the McMillan equation [33]:

$$\lambda_{e-ph} = \frac{\mu^* \ln\left(\frac{\Theta_D}{1.45T_c}\right) + 1.04}{\ln\left(\frac{\Theta_D}{1.45T_c}\right)(1 - 0.62\mu^*) - 1.04} \quad (2)$$

where  $\mu^*$  is Coulomb pseudopotential and is often set to 0.15 as the empirical value. From the estimation we get  $\lambda_{e-ph} = 0.69$ . This value is less than the minimum value 1 of strong coupling, which suggest it is still in an intermediate coupling range. The density of states at the Fermi level  $N(E_F)$  can be calculated by the equation:

$$N(E_F) = \frac{3\gamma}{\pi^2 k_B^2 (1 + \lambda_{e-ph})} \quad (3)$$

$N(E_F) = 1.53$  state/eV f.u. for our sample. This value is close to that of undoped  $2H-TaSe_2$  which is 1.51 state/eV f.u., but lower than those of other doped or intercalated  $TaSe_2$  which are about 2 state/eV f.u. [21]. In general, high  $N(E_F)$  is in favor of superconductivity. In spite of having low  $N(E_F)$ ,  $4Ha-Ta_{1.03}Se_2$  also has comparable  $T_c$  to other doped or intercalated  $TaSe_2$ , indicating that the stacking mode of  $4Ha$  may be in favor of superconductivity than other polytypes.

#### 4. Conclusion

In summary, we discover superconductivity with an onset  $T_c$  of 2.7 K in the Ta self-intercalated  $4Ha-Ta_{1.03}Se_2$ . A suppressed CDW transition is observed around 106 K. A kind of special stacking faults is revealed, which may increase the anisotropy. The

$\mu_0 H_{c2}^{ab}(0)/T_c = 4.48$  is larger than other polytypes, and the estimated  $H_{c2}^{ab}(0)$  is 2.44 times of the Pauli paramagnetic limit, which may result from enhanced SOC.  $\lambda_{e-ph} = 0.69$ , indicating that it is still in the intermediate coupling range. On the other hand,  $N(E_F)$  is only 1.53 state/eV f.u., smaller than that of other doped or intercalated  $TaSe_2$ , but  $T_c$  is almost the same as them. This work indicates that the stack mode of  $4Ha$  polytype is of benefit to superconductivity and  $H_{c2}$  for  $TaSe_2$ , and superconductivity could be even enhanced if  $N(E_F)$  can be increased.

#### 5. Acknowledgments

We thank Yi Zhou and Guanghan Cao for helpful discussions. This work was supported by the National Basic Research Program of China (Grant Nos. 2014CB92103) and the National Key R&D Projects of China (Grant No. 2016FYA0300402), the National Science Foundation of China (Grant Nos. U1332209 and 11774305), and the Fundamental Research Funds for the Central Universities of China. We thank the Center of Electron Microscopy of ZJU for the access to microscope facilities used in this work. We also thank Lei Qiao for the help on using the Ultra Low Field option in the magnetic measurements.

#### 6. References

- [1] Morris R, Coleman R and Bhandari R 1972 *Phys. Rev. B* **5** 895
- [2] Suzuki N, Yamamoto A and Motizuki K 1984 *Solid State Commun.* **49** 1039
- [3] Ali M N *et al.* 2014 *Nature* **514** 205
- [4] Deng K *et al.* 2016 *Nat. Phys.* **12** 1105
- [5] Katzke H, Tolédano P and Depmeier W 2004 *Phys. Rev. B* **69** 134111
- [6] Morosan E, Zandbergen H W, Dennis B S, Bos J W G, Onose Y, Klimczuk T, Ramirez A P, Ong N P and Cava R J 2006 *Nat. Phys.* **2** 544
- [7] Li L J, O'Farrell E C, Loh K P, Eda G, Özyilmaz B and Castro Neto A H 2016 *Nature* **529** 185
- [8] Yu Y J, Yang F Y, Lu X F, Yan Y J, Cho Y H, Ma L G, Niu X H, Kim S, Son Y W and Feng D L 2015 *Nat. Nanotechnol.* **10** 270
- [9] Freitas D *et al.* 2016 *Phys. Rev. B* **93** 184512
- [10] Moliniè P, Jérôme D and Grant A J 1974 *Philos. Mag.* **30** 1091
- [11] Liu Y *et al.* 2016 *Phys. Rev. B* **94** 045131
- [12] Liu Y, Ang R, Lu W J, Song W H, Li L J and Sun Y P 2013 *Appl. Phys. Lett.* **102** 192602
- [13] Ang R, Miyata Y, Ieki E, Nakayama K, Sato T, Liu Y, Lu W J, Sun Y P and Takahashi T 2013 *Phys. Rev. B* **88** 115145
- [14] Moncton D E, Axe J D and DiSalvo F J 1977 *Phys. Rev. B* **16** 801
- [15] Fleming R M, Moncton D E, McWhan D B and DiSalvo F J 1980 *Phys. Rev. Lett.* **45** 576
- [16] Kumakura T, Tan H, Handa T, Morishita M and Fukuyama H 1996 *Czech. J. Phys.* **46** 2611
- [17] Yokota K, Kurata G, Matsui T and Fukuyama H 2000 *Physica B* **284** 551

- [18] Li L J *et al.* 2017 *Npj Quantum Mater.* **2** 11
- [19] Luo H X, Xie W W, Tao J, Inoue H, Gyenis A, Krizan J W, Yazdani A, Zhu Y M and Cava R J 2015 *Proc. Natl. Acad. Sci. USA* **112** E1174
- [20] Li L J, Sun Y P, Zhu X D, Wang B S, Zhu X B, Yang Z R and Song W H 2010 *Solid State Commun.* **150** 2248
- [21] Bhoi D, Khim S, Nam W, Lee B S, Kim C, Jeon B G, Min B H, Park S and Kim K H 2016 *Sci. Rep.* **6** 24068
- [22] Bjerkelund E and Kjekshus A *Acta Chem. Scand.* **21** 513
- [23] Luo H X, Xie W W, Seibel E M and Cava R J 2015 *J. Phys.: Condens. Matter.* **27** 365701
- [24] Di Salvo F J, Moncton D E, Wilson J A and Mahajan S 1976 *Phys. Rev. B* **14** 1543
- [25] Fung K K, Steeds J W and Eades J A 1980 *Physica B + C* **99** 47
- [26] Liu Y, Li L J, Lu W J, Ang R, Liu X Z and Sun Y P 2014 *J. Appl. Phys.* **115** 043915
- [27] Liu Y, Lu W J, Li L J, Zhu X D, Song W H, Ang R, Ling L S, Liu X Z and Sun Y P 2015 *J. Appl. Phys.* **117** 163912
- [28] Bjerkelund E K A 1967 *Acta Chem. Scand.* **21** 513
- [29] Werthamer N R, Helfand E and Hohenberg P C 1966 *Phys. Rev.* **147** 295
- [30] Zhang Q, Li G, Rhodes D, Kiswandhi A, Besara T, Zeng B, Sun J, Siegrist T, Johannes M D and Balicas L 2013 *Sci. Rep.* **3** 1682
- [31] Zhou N *et al.* 2014 *Phys. Rev. B* **90** 094520
- [32] Chen Q, Yang X, Yang X, Chen J, Shen C, Zhang P, Li Y, Tao Q and Xu Z A 2017 *Front. Phys. China* **12** 127402
- [33] McMillan W L 1968 *Phys. Rev.* **167** 331